On Ambiguities in SAR Design

Anthony Freeman, Jet Propulsion Laboratory, USA

Abstract

Ambiguities are an aliasing effect caused by the periodic sampling of the scene backscatter inherent to pulsed radar systems such as Synthetic Aperture radar (SAR). In this paper we take a fresh look at the relationship between SAR range and azimuth ambiguity constraints on the allowable pulse repetition frequency (PRF) and the antenna length. We show that for high squint angles smaller antennas may be feasible in some cases.

For some applications, the ability to form a synthetic aperture at high squint angles is desirable, but the size of the antenna causes problems in the design of systems capable of such operation. This is because the SAR system design is optimized for a side-looking geometry. In two examples design examples we take a sub-optimum antenna size and examine the performance in terms of azimuth resolution and swath width as a function of squint angle. We show that for stripmap SARs, the swath width is usually worse for off-boresight squint angles, because it is severely limited by range walk, except in cases where we relax the spatial resolution. We consider the implications for the design of modest-resolution, narrow swath, scanning "SAR scatterometers".

1 Introduction

In an earlier paper [1] we examined the familiar SAR antenna area constraint and showed that it was actually a 'soft' constraint, in that SAR systems can and have been operated with antennas smaller than this constraint would normally allow. We showed that this design rule only applies when the SAR system engineer seeks to achieve maximum swath width and

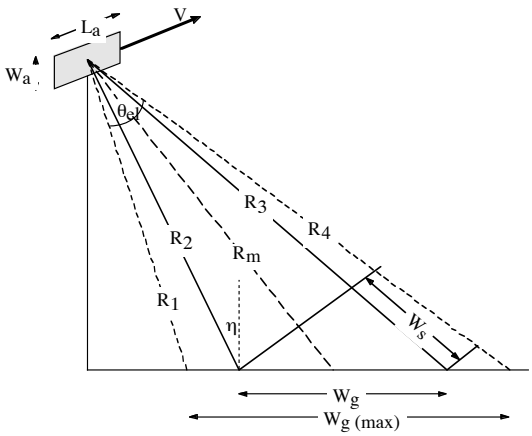

Figure 1: Side-looking SAR Imaging Geometry

minimum possible azimuth resolution at the same time. If a smaller swath and/or degraded azimuth resolution is acceptable, then it is possible to use a smaller antenna (or to use a lower PRF when operating). The result in [1] does not provide infinite flexibility in SAR system design: for example, the lowest PRF possible is about 70% of the Doppler bandwidth, and results in significantly degraded azimuth resolution.

The analysis presented in [1] followed convention in the literature in that it was developed for a side-looking geometry, in which the SAR antenna is pointed at a 90 degree azimuth angle with respect to the flight track of the platform. The side-looking geometry of Figure 1 is attractive to designers of SAR imagers because it produces point spread functions (PSF's) in ground range and along-track dimensions which are orthogonal. Orthogonal PSF's lead to rectangular resolution cells, and visually pleasing images that are considered easier to interpret.

In this paper, we further examine the assumptions that lead to the minimum SAR antenna area constraint. We show that the constraint needs to be modified for squint angle geometry, and that smaller antennas can be used that still allow the SAR designer to avoid significant azimuth ambiguity levels by sampling at higher than the Doppler bandwidth. At higher squint angles, the result is a highly distorted SAR image. However, this may be less important for designers of SAR interferometer systems, for example, for which the SAR image representing backscatter is less relevant, in comparison with the phase information obtained by comparing phases of images acquired on different passes. Distorted images are also less important for imaging systems with modest swath width/resolution requirements, such as scanning "SAR scatterometers".

2 PRF Constraints

After [1], to control range ambiguities we need:

$$PRF < c/(2W_g \sin\eta) \quad (1)$$

i.e. the pulse repetition frequency must be smaller than the time it takes to collect returns from the entire illuminated swath (assuming that we seek to take advantage of all of the available swath width). This ignores the addition requirement to add the overhead of the transmit pulse, which we shall incorporate later. From [2], the constraint on the PRF to avoid azimuth ambiguities is:

$$PRF > B_D \quad (2)$$

where B_D is the Doppler bandwidth which is the range of Doppler frequencies extending across the antenna footprint. The Doppler bandwidth is generally given as:

$$B_D = 2V_{st}/L_a \quad (3)$$

However, this is a simplification of the general case for the case when squint angle θ = 0. For a non-zero squint angle (Fig. 2), the appropriate expression is [3]:

$$B_D = \frac{2V_{st}}{\lambda}\left[\sin(\theta + \delta\theta/2) - \sin(\theta - \delta\theta/2)\right] \quad (4)$$

where $\delta\theta = \lambda/L_a$ is the antenna azimuth beamwidth. For small beamwidths, $\delta\theta$, eq. (4) approximates to:

$$B_D \approx \frac{2V_{st}}{L_a}\cos\theta \quad (5)$$

Eq. (4) approximates to (3) only when θ = 0. For high squint angles, the Doppler bandwidth is, therefore, significantly less than the limit given in (3).

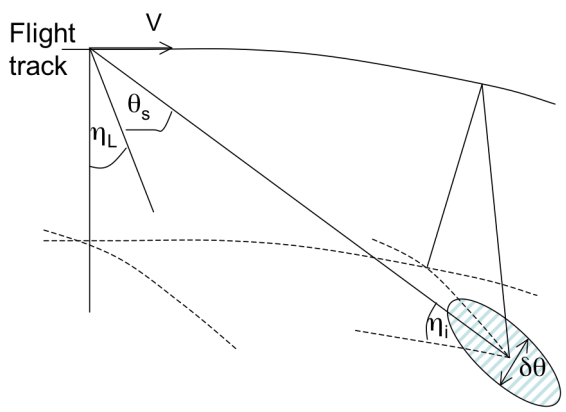

Figure 2: Squinted viewing geometry

This is significant, for the upper limit on the PRF given in (1) is *independent* of the squint angle. Thus any flexibility we may have in selecting the PRF lies in the lower limit, which seeks to control azimuth ambiguities caused by Doppler aliasing.

Next we derive a revised version of the SAR antenna area constraint, taking into account the squint angle. Starting with the expression for the maximum illuminated swath projected from the look direction onto the ground [1], i.e.

$$W_g(\max) = \frac{\lambda R}{W_a \cos\eta} \quad (6)$$

and combining it with the constraints expressed in (1) and (5), we obtain:

$$W_a L_a \geq \frac{4V_{st}\lambda R}{c} \tan\eta \cos\theta \quad (7)$$

We can now turn the design problem around and ask: if we have a fixed (small) antenna, is there a range of squint angles over which we can find a PRF that is consistent with both of the upper and lower limits expressed in (1) and (2)? So that antenna can then be used to generate SAR imagery with acceptable ambiguity levels?

3 System Design Examples

3.1 L-Band Stripmap SAR

Let us apply the foregoing to an example system design. We set out to design an L-Band stripmap SAR system with the characteristics described in Table 1. We select an L-Band system because the conventional SAR design approach, applying the minimum SAR antenna area constraint, typically results in antennas that are huge structures ~10 x 2.5 m in size.

Parameter	Value
Wavelength	0.24 m
Spatial resolution	100m
Swath width	75 km
# of looks	64
Noise-equivalent σ^o	-30 dB
Incidence angle	30 degrees
Ambiguity levels	< -20 dB
Antenna dimensions	4 m x 2.5 m
Orbit altitude	600 km

Table 1: SAR image product characteristics

Figure 3 shows the PRF limits for the system characterized in Table 1. Note that there are no PRF's that allow full swath coverage for this system at zero

squint angle – we have to look off-boresight to find a viable operating range, though we shall also see that the swath width is less than that at boresight.

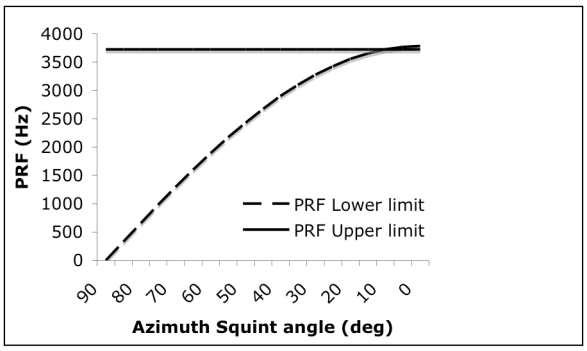

Figure 3: Upper and lower limits on the PRF as a function of squint angle

Having found that there exists a range of squint angles for a 4 x 2.5 m antenna with a valid PRF, the next question to answer is whether such a system can provide an adequate noise floor (i.e. SNR)? Using an appropriate expression for SAR Noise-equivalent sigma-zero from [2] we find that the requirements given in Table 1 can nearly all be met with the system specifications given in Table 2. The exception is swath width, which is discussed below. The range of parameters presented in Table 2 are reasonable – they do not stretch the bounds of what is possible in SAR system design.

Parameter	Value
Swath width	42 km
Squint angle	30 degrees
Bandwidth	12.5 MHz
Peak transmit power	5 kW
Pulse length	10 μs
PRF	4535 Hz
# of bits/sample	5
Data rate	150 Mbps
Noise floor	< - 30 dB
# of looks	80

Table 2: SAR system characteristics

To calculate the actual width of the strip map swath achievable for a given squint angle, we used a modified version of the expression for the swath width (from equation (27) in [3]):

$$W_s < \frac{c}{2}\left[\frac{\cos\theta}{PRF} - 2\tau_p\right] + \left[c\tau_p(1-\cos\theta) - \frac{\lambda R}{2\Delta_{az}}\tan\theta\right] \quad (8)$$

where τ_p is the pulse length. In the final term in this expression we have substituted $2\Delta_{az}$ for the aperture length, L_a. This is to take into account the range walk only over the time needed to generate a synthetic aperture to provide the required (best-case) azimuth resolution Δ_{az}. This helps prevent the range walk term from dominating when we evaluate (8). In Figure 4 we plot the swath width (projected onto the ground) as a function of squint angle for the system described in Tables I and II. The figure shows that the system generally provides reduced swath at high squint angles. The effect is predominantly caused by the range walk term in eq. (8), which can be quite large for high squint angles. However, if the SAR designer can trade off best-case azimuth resolution (or number of looks in the final 100 m data product), this effect can be reduced significantly, as shown in the Figure (Cases II and III).

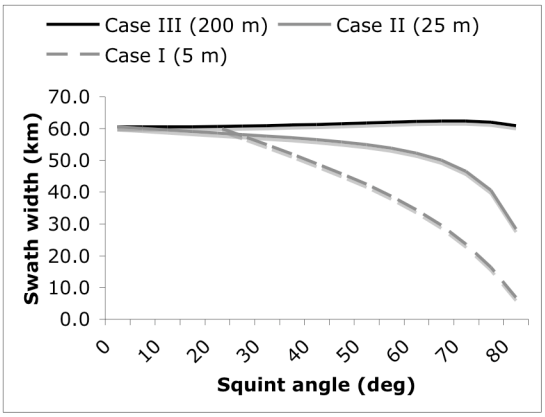

Figure 4: Swath width versus squint angle for 3 cases: Δ_{az} = 5 m (I), Δ_{az} = 25 m (II), and Δ_{az} = 200 m (III)

Note that what we choose to plot in Figure 4 is the swath achievable within an interpulse period, with the PRF set at 1.2 x Doppler Bandwidth for each squint angle (for minimum azimuth resolution). At zero squint angle this produces a swath width of 60 km which is less than the illuminated swath, as in [1]. Only when we minimize the range walk contribution in (8) by aiming for significantly degraded azimuth resolution (as in Case III), do we see swath widths greater than 60 km.

3.2 P-Band UHF Scanning System

Next we seek to design a P-Band SAR system with the characteristics described in Table 3. This system scans through 2π radians every 40 seconds at a constant incidence angle of 30 degrees.

Parameter	Value
Wavelength	0.68 m
Spatial resolution	100m
Swath width	30 km
Antenna rotation rate	2.7 rpm
Rotation period	40 s
Swath coverage	540 km
Noise-equivalent σ^o	-35 dB
Incidence angle	30 degrees
Repeat period	49 days
Antenna dimensions	6 m x 6 m
Orbit altitude	800 km

Table 3: P-Band system characteristics

Figure 5 shows the swath limits for the system characterized in Table 1 as a function of cross-track distance from the nadir track.

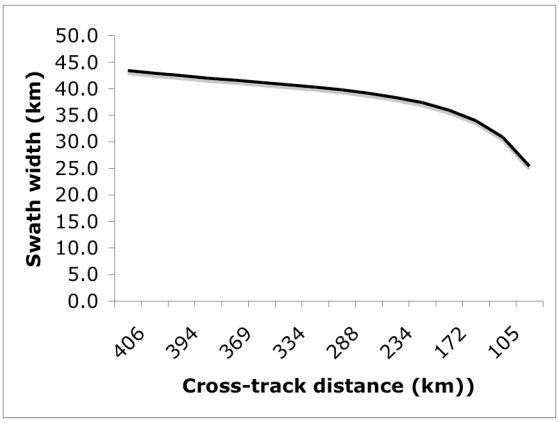

Figure 5: Swath width vs. Cross-track distance for the P-Band system

The figure shows that the usable swath coverage (for a 30 km instantaneous swath) is ~270 km on each side of nadir, or 540 km in total. The rotation period specified in Table 3 is too long for contiguous coverage as defined in [4]; space in between swaths will have to be filled in on successive passes. With this set-up, however, it is possible to acquire global coverage in 49 days – twice as fast when compared with a strip mapping approach using a 30 km swath.

4 Implications

We have shown that, to first order, it is possible to obtain acceptable performance for a squinted SAR system with a smaller antenna than is conventionally adopted for a side-looking system. We still need to confirm through a rigorous ambiguity analysis that the system requirement of ambiguities less than -20 dB can be met.

The 40 km swath achieved in the L-band stripmap SAR system design example was worse than the side-looking case and did not meet the requirement. It may be too small for many applications. We can achieve a slightly wider swath off-boresight [as suggested by (7)] if we minimize the range walk contribution to (8) by aiming for degraded azimuth resolution. This means we have to trade off spatial resolution or number of looks in the final image product. To further extend the swath coverage it may be possible to use ScanSAR with a squinted SAR system, mapping out sub-swaths to cover a wide area, and operating in burst mode. The usual trade-off between azimuth resolution and/or number of looks should apply.

Smaller antennas may be useful in the class of radar remote sensing instruments we will call SAR scatterometers [4], as shown in the P-Band example. SAR scatterometers scan through a range of squint angles and are often designed with small swath widths (a few 10's of km), but have a requirement for finer resolution (typically 100's of m to km's) than the real aperture antenna may offer. Synthetic aperture techniques offer a way to achieve such resolution, but if the antenna is optimized for operation in conventional side-looking mode, it may be too large. According to the results in this paper, smaller antennas may be used in such systems, to provide the required performance over a range of squint angles.

A smaller antenna has considerable advantages in mass and ease of deployment. It could fit in most launch shrouds without the need for hinging or a deployment mechanism. Using current phased array antenna technology, a mass per unit area of roughly 10 kg/sq. m is achievable. A 4 x 2.5 m antenna, for example, could weigh in at just 100 kg, instead of 250 kg for a 10 x 2.5 m antenna, a considerable mass saving. Additional savings may be realized because we can omit the antenna deployment mechanism. The mass saving may be even greater if a reflector antenna were used instead, with mass/unit area < 3 kg/sq. m. Current projections for antenna technology developments suggest that we will have to wait a considerable period for very low-mass inflatable and/or membrane antennas to be available to achieve comparable mass savings for a full-size antenna. A disadvantage of a squinted antenna is the increased drag on the Spacecraft, in comparison with a true side-looking antenna.

Acknowledgements

The research described in this paper was carried out by the Jet Propulsion Laboratory, California Institute of Technology, under a contract with the National Aeronautics and Space Administration.

References

[1] A. Freeman, W. T. K. Johnson, B. Honeycutt, R. Jordan, S. Hensley, P. Siqueria, and J. Curlander, "The myth of the minimum SAR antenna area constraint," IEEE Trans. Geosci. Remote Sensing, vol. 38, pp. 320–324, Jan. 2000.

[2] SAR Systems and Processing, Curlander, J.C. and McDonough, R. N., publ. J. Wiley, 1991.

[3] Davidson, G. and Cummings, I., Signal Properties of Spaceborne Squint-Mode SAR, IEEE TGRS, Vol. 35, No. 3, May 1997.

[4] Spencer,, M.W., Tsai, W. and Long, D.G., High-Resolution Measurements With a Spaceborne Pencil-Beam Scatterometer Using Combined Range/Doppler Discrimination Techniques, IEEE TGRS Vol. 41, No. 3, March 2003.